Functional Integrity in Children With Anoxic Brain Injury From Drowning

Mariam Ishaque,[1,2]* Janessa H. Manning,[3] Mary D. Woolsey,[1] Crystal G. Franklin,[1] Elizabeth W. Tullis,[4] Christian F. Beckmann,[5,6,7] and Peter T. Fox [1,2,8,9]*

[1]*Research Imaging Institute, University of Texas Health Science Center at San Antonio, San Antonio, Texas*
[2]*Department of Radiology, University of Texas Health Science Center at San Antonio, San Antonio, Texas*
[3]*Merrill Palmer Skillman Institute, Wayne State University, Detroit, Michigan*
[4]*Conrad Smiles Fund, San Antonio, Texas*
[5]*Department of Cognitive Neuroscience, Radboud University Medical Center, Donders Institute for Brain, Cognition and Behaviour, Nijmegen, The Netherlands*
[6]*Donders Institute for Brain, Cognition and Behaviour, Donders Center for Cognitive Neuroimaging, Radboud University, Nijmegen, The Netherlands*
[7]*Centre for Functional MRI of the Brain, University of Oxford, Oxford, United Kingdom*
[8]*South Texas Veterans Healthcare System, San Antonio, Texas*
[9]*Shenzhen University School of Medicine, Shenzhen, People's Republic of China*

Abstract: Drowning is a leading cause of accidental injury and death in young children. Anoxic brain injury (ABI) is a common consequence of drowning and can cause severe neurological morbidity in survivors. Assessment of functional status and prognostication in drowning victims can be extremely challenging, both acutely and chronically. Structural neuroimaging modalities (CT and MRI) have been of limited clinical value. Here, we tested the utility of resting-state functional MRI (rs-fMRI) for assessing brain functional integrity in this population. Eleven children with chronic, spastic quadriplegia due to drowning-induced ABI were investigated. All were comatose immediately after the injury and gradually regained consciousness, but with varying ability to communicate their cognitive state. Eleven neurotypical children matched for age and gender formed the control group. Resting-state fMRI and co-registered T1-weighted anatomical MRI were acquired at night during drug-aided sleep. Network integrity was quantified by independent components analysis (ICA), at both group- and per-subject levels. Functional-status assessments based on in-home observations were provided by families and caregivers. Motor ICNs were grossly compromised in ABI patients both group-wise and individually, concordant with their prominent motor deficits. Striking preservations of perceptual and cognitive ICNs were observed, and the degree of network preservation correlated ($\rho = 0.74$) with the per-subject functional status assessments. Collectively, our findings indicate that rs-fMRI has promise for assessing

Additional Supporting Information may be found in the online version of this article.

Contract grant sponsor: National Center for Advancing Translational Sciences; Contract grant number: TL1 TR001119; Contract grant sponsor: National Institutes of Health; Contract grant number: TL1 TR001119; Contract grant sponsor: National Institute of Mental Health; Contract grant number: R01 MH074457; Contract grant sponsor: Kronkosky Charitable Foundation

*Correspondence to: Mariam Ishaque and Peter T. Fox; 7703 Floyd Curl Drive, San Antonio, TX 78229, USA. E-mails: Ishaque@livemail.uthscsa.edu and Fox@uthscsa.edu

Received for publication 2 June 2016; Revised 10 July 2017; Accepted 15 July 2017.

DOI: 10.1002/hbm.23745

Published online 31 July 2017 in Wiley Online Library (wileyonlinelibrary.com).

brain functional integrity in ABI and, potentially, in other disorders. Furthermore, our observations suggest that the severe motor deficits observed in this population can mask relatively intact perceptual and cognitive capabilities. *Hum Brain Mapp 38:4813–4831, 2017.*

Key words: anoxic brain injury; locked-in syndrome; minimally conscious state; functional magnetic resonance imaging; hypoxic–ischemic encephalopathy; independent components analysis; neural networks; resting state; fMRI; rs-fMRI; rs-fcMRI

INTRODUCTION

Drowning is the second most prevalent cause of unintentional injury death in children 1–4 years of age. Nonfatal drowning (i.e., cardiopulmonary resuscitation is successful) is prevalent in this age group, with an estimated 2 out of 3 drowned children surviving [Borse and Sleet, 2009; Kriel et al., 1994; Topjian et al., 2012]. Neurological morbidity from anoxic brain injury (ABI) is a frequent outcome, as the brain is exquisitely sensitive to oxygen deprivation [Topjian et al. 2012].

Functional assessment and prognostication are extremely challenging in this disorder, both acutely and chronically. In the acute state, victims are typically comatose and may remain unresponsive for weeks. Acutely, T1- and T2-weighted MRI are often normal or suggest diffuse swelling; chronically, diffuse atrophy is the most frequently reported finding [Rafaat et al., 2008; Rabinstein and Resnick, 2009]. When focal pathology is present, basal ganglia and cerebellar damage are the most commonly reported and both are associated with poor outcomes [Rabinstein and Resnick, 2009]. In the chronic state, spastic quadriparesis resembling severe cerebral palsy is the most common presentation. This entails loss of self-mobility, self-feeding, and verbal communication with various movement disorders being reported [Lu-Emerson and Khot, 2010]. Children with anoxic brain damage are frequently deemed to be in a minimally conscious or vegetative state, but these determinations may well be flawed, as communication and task-cooperation limitations often preclude reliable assessment of cognitive status [Ibsen and Koch, 2002; Childs et al., 1993; Levy et al., 1985; Topjian et al., 2012].

The neuropathology of pediatric, nonfatal ABI is not well established. Postdrowning anoxic injury has been described as diffusely affecting grey matter more than white matter, reflecting the respective metabolic demands of the two tissue types [Huang and Castillo, 2008; Rabinstein and Resnick, 2009]. However, the possibility of a more selective injury must be considered in view of the predominant motor-system disability observed in survivors. Until recently, structural imaging methods had contributed little to our understanding of the disorder. The limited utility of these methods stemmed chiefly from the use of standard, clinical acquisition protocols which were not optimized for this condition (the neuropathology of which was unknown), compounded by a reliance on visual inspection for image interpretation (i.e., on nonquantitative methods) [Guttierrez et al., 2010; Howard et al., 2011; Huang and Castillo, 2008; Topjian et al., 2012]. In the same patient cohort reported here, our group recently reported quantitative analyses of two structural imaging modalities. Voxel-based morphometry (VBM) was applied to T1-weighted MRI to independently quantify grey and white matter tissue loss [Ishaque et al., 2016]. Grey matter loss was largely restricted to the basal ganglia and thalamus; white matter loss predominately affected the posterior limb of the internal capsule (PLIC). Tract-based spatial statistics (TBSS) was applied to diffusion-weighted MRI to quantify fractional anisotropy and mean diffusivity [Ishaque et al., 2017]. TBSS independently confirmed our VBM white-matter findings, also showing highly focal, deep subcortical lesions. Furthermore, per-subject motor-function scores correlated highly with both fractional anisotropy (Spearman's $\rho = 0.8$) and mean diffusivity ($\rho = -0.83$) in the PLIC. For both modalities, the lesion was largely confined to the lenticulostriate vascular distribution, suggesting that this end-arterial watershed zone may be uniquely susceptible in young children. A similar distribution has been reported in perinatal asphyxia using diffusion tensor imaging (DTI) [Barkovitch et al., 2001] and magnetic resonance spectroscopy [Pu et al., 2000], lending further credence to this hypothesis. Descending corticospinal and corticobulbar fibers (pyramidal tract) pass through the PLIC, the cerebral peduncles (midbrain) and anterior pons *en route* to the pyramidal decussation (medulla). Collectively, these observations suggest that pediatric drowning victims may be an at-risk population for a selective deefferentation syndrome, with disproportionate motor impairment and relatively preserved perceptual and cognitive function. To test this hypothesis, we implemented rs-fMRI and quantitative behavioral assessments in the same pediatric ABI cohort in this study.

In pediatric brain injury, traditional, task-activation fMRI is extremely difficult to implement reliably [Munson et al., 2006]. Resting-state fMRI is a task-free alternative that has been widely used in adult populations unable to comply with in-scanner tasks. Resting-state fMRI, however, is notoriously susceptible to movement artifacts [Power et al. 2014], which poses a substantial obstacle for pediatric studies, in general, and for pediatric brain injury, in particular.

Sleep has been successfully used in pediatric populations to achieve in-scanner immobility for anatomical MRI [Giedd et al., 1999], task-activation fMRI (using auditory stimuli) [Anderson et al., 2001; Redcay and Courchesne, 2008], and during resting-state fMRI [Manning et al., 2013]. In prior work from our laboratory, we demonstrated that intrinsic connectivity networks (ICNs) persist during natural, nocturnal sleep in pre-school-aged neurotypical children [Manning et al., 2013]. In that study, we applied independent components analysis (ICA), a whole-brain (i.e., not region-of-interest based), voxel-wise, data-driven procedure that extracts functionally connected networks by temporal coherence of spontaneous fluctuations in T2* signal [Beckmann and Smith, 2004; Beckmann et al., 2005]. ICNs are known to persist during natural sleep [Fukunaga et al., 2006; Horovitz et al., 2008; Manning et al., 2013] and sedation [Peltier et al., 2005; Vincent et al., 2007]. Importantly, the canonical, discrete ICNs extracted with ICA [Smith et al., 2009] correlate to more-or-less discrete behavioral domains and task-activation paradigms [Laird et al., 2009, 2011] facilitating correlations with behavioral assessments. ICNs also predict individual differences in task-activation fMRI effects [Tavor et al., 2016], making them a suitable alternative in populations not able to comply with task-activation protocols. An acquisition, analysis, and interpretation strategy combining the approaches of Manning, Smith, and Laird was applied here.

Quantitative behavioral assessments were obtained via structured interviews with families and caregivers using Likert-style questionnaires developed for this population and designed to correspond to canonical ICA-derived ICNs. Caregiver assessments were used because (1) families have knowledge of the patients' premorbid personalities, habits, and preferences which could help them recognize coherent response patterns; (2) families and care staff have extensive opportunities for observation and interaction with patients; and (3) caregivers are accessible to the research team and accepting of the time demands involved. Additional motivation for this approach came from evidence that family and care staff are most often the first to recognize the return of awareness in locked-in syndrome (LIS) and other disorders of consciousness (Leon-Carrion et al., 2002; Smith and Delargy, 2005; Owen, 2017).

For the data reported here, 11 children with chronic postdrowning ABI and 11 neurotypical controls matched for age and gender were imaged during nocturnal, drug-aided sleep, acquiring both rs-fMRI (BOLD) and structural MRI (T1-weighted). ICA was implemented both group-wise and per-subject at a dimensionality of 20. From these 20 networks, 11 canonical networks were identified: five perceptual networks (Visual × 3, Auditory, Sensorimotor); two motor networks (basal ganglia, cerebellum); and four cognitive networks (default mode, executive function, left and right frontoparietal). We hypothesized that (1) resting-state fMRI would demonstrate group-level differences between these cohorts, (2) resting-state fMRI would demonstrate per-patient abnormalities, (3) imaging-based results would be concordant with behavioral results, and (4) motor-network abnormalities would greatly outweigh perceptual- and cognitive-network abnormalities.

MATERIALS AND METHODS

Participants

ABI subjects were recruited by means of collaborations with the Nonfatal Drowning Registry (nonfataldrowningresigstry.org), the Conrad Smiles Fund (https://ww.R-project.org/), and Miracle Flights (miracleflights.org). Families of drowning victims were made aware of the study via the Nonfatal Drowning Registry, to which they had previously provided contact information. Interested families initiated contact with the study project coordinator at the University of Texas Health Science Center, San Antonio for screening and enrollment. Ten of the recruited ABI victims resided in North America; one ABI victim resided in Europe. The North American participants were widely geographically dispersed, with most travelling thousands of miles (i.e., from the East and West Coasts) to participate. Air-travel costs were subsidized by Miracles Flights; lodging costs were subsidized by the Conrad Smiles Fund. No other monetary incentives were provided. In all instances, the parents' primary motivation for participation was to better understand their child's neurological and cognitive status. In keeping with this expectation, parents were provided with a formal report of their child's imaging and behavioral results at the completion of the study. Available funding limited the scope of enrollment to 11 ABI victims and 11 controls. Controls were recruited chiefly from friends and family of patients. The study's protocol was approved by the University of Texas Health Science Center at San Antonio's Institutional Review Board, in compliance with the Code of Ethics of the World Medical Association (Declaration of Helsinki). Informed consent was obtained from the participants' parent(s). Per-patient descriptions are provided as Supporting Information (SI) for the 10 patients with good-quality imaging data. In the following, we make reference to patient identification numbers provided in the SI.

Medical history

Medical history was taken at the time of scan acquisition and supplemented by video-conference structured interviews subsequent to scanning (described below in Quantitative Behavioral Assessment). All ABI participants had accidentally drowned in early childhood (age at injury: 17–48 months); had been pulseless and apneic at the scene; had been administered cardiopulmonary resuscitation and cardioversion by emergency medical technicians *en route* to the hospital; had been admitted to the hospital in a comatose state; had required intubation and mechanical

TABLE I. Patient characteristics

	Gender	Age at injury (months)	Age at study (years)	Acute MRI	Acute care recommendation	Clinical categorization
P1	Male	21	5	Global injury	Withdraw care	Classical LIS
P2	Male	36	5	Unknown	Withdraw care	Incomplete LIS
P3	Male	48	6	Global injury	Withdraw care	Incomplete LIS
P4	Female	17	5	Normal	Withdraw care	Complete LIS/MCS+
P5	Female	36	8	Diffuse Edema	Withdraw care	Complete LIS/MCS+
P6	Female	24	7	Normal	Proceed with treatment	Classical LIS
P7	Male	20	4	Normal	Proceed with treatment	Incomplete LIS
P8	Male	36	11	Global injury	Withdraw care	Incomplete LIS
P9	Male	24	11	Diffuse edema	Withdraw care	Incomplete LIS
P10	Male	17	12	Normal	Institutionalize	Complete LIS/MCS+

For the ABI patient cohort, the gender, age at injury (months), age at behavioral and imaging assessment (years), results of MRI at hospital admission, acute care recommendation, and clinical categorization are shown. Clinical categorizations use the terminologies of Bauer et al. (1979) and Bruno et al. [2009].

ventilation; had been treated for cerebral swelling (e.g., with steroids or hypothermia); and had protracted hospital stays. In the acute setting, most (7/10) were advised by the medical team to withdraw care but opted not to follow this guidance. All transitioned from coma through a minimally conscious state to a state in which the caregivers believed that the patients were conscious and aware of themselves and their environment. At the time of study participation, all were at least 6 months postinjury, were not mechanically ventilated, and were being cared for in the parents' home. All had normal sleep–wake cycles and were attentive to their environment. Nine had permanent gastric tubes for feeding, being unable to safely take food by mouth. Most had difficulty swallowing saliva and required periodic suctioning (Table I).

Neurological assessment

Neurological examination was performed by a neurologist (PTF), at the time of scan acquisition. All ABI participants had severe, spastic quadriplegia with involvement of neck and facial musculature, indicative of a supranuclear, corticospinal tract lesion. All were awake, alert, and attentive to the environment but had little (3 patients) or no intelligible speech (7 patients). Using published clinical diagnostic criteria [Bauer et al., 1979; Bruno et al., 2011; Laureys et al., 2004; Plum and Posner, 1982] for LIS and minimally conscious state (MCS), these patients were clinically categorized as Classical LIS (2 patients), as Incomplete LIS (5 patients) and as somewhere on the spectrum of MCS+ to Total LIS (3 patients). Two patients (Patients 1 and 6) had Classic LIS, communicating effectively by eye movements. Five patients (Patients 2, 3, 7, 8, and 9) were clinically categorized as Incomplete LIS. Of these, two (Patients 2 and 9) were clinically categorized as Incomplete LIS because they had some limb movement and communicated by pointing or button pressing. Three were categorized as Incomplete LIS in that they have some limited, effortful speech (Patients 3, 7, and 8); of these, two also had some limb movement (Patients 3 and 7). Even in these Incomplete LIS patients, however, the predominant mode of communication was eye gaze (Patients 2, 7, 8, and 9) or nonspeech sounds (Patient 3), reflecting the severity of their deefferentation. Two patients (Patients 7 and 9) made use of eye-gaze-controlled computer interfaces to communicate; one of these (Patient 9) read electronic books via an eye-gaze-controlled system and communicating by spelling. Three patients (Patients 4, 5, and 10) were clinically classified as Total LIS or MCS+, being quadriplegic, aphonic, awake (sustained eye opening), and aware of their environment (aware of touch, voice and other sounds, etc.) but being unable to communicate effectively by eye movements or gesture. Per-patient descriptions and clinical categorizations are provided in Supporting Information.

Quantitative Behavioral Assessment

Quantitative behavioral assessments were performed using both normed, published instruments designed for cerebral palsy (cerebralpalsy.org.au) and non-normed, in-house instruments designed for this patient population. The four published instruments were Gross Motor Function Classification System (GMFCS) [Palisaono et al., 1997]; Manual Ability Classification System (MACS) [Eliasson et al., 2006; Communication Function Classification System (CFCS) [Hidecker et al., 2011; and, Eating and Drinking Ability Classification System (EDACS) [Sellers et al., 2014]. All measures are Likert-type scales rated 1–5. Assessments using these four instruments were completed during the patient's visits to the Research Imaging Institute at the University of Texas Health Science Center at San Antonio. These instruments proved of limited value for several reasons. First, the severity of the motor deficits caused floor effects on three of these measures (GMFCS, MACS, and EDACS). Specifically, 10 patients scored V (i.e., worst score) in GMFCS, MACS, and EDACS, despite having a

discernible range in abilities; one patient scored IV on each instrument. Second, the measures did not include assessments for perceptual abilities (vision, audition, somesthesis), as these are not typically impaired in cerebral palsy. As perceptual networks feature prominently in ICN analyses, quantitative assessments of perceptual abilities were needed for the planned imaging–behavior correlation analysis. Third, the communication assessment was not sufficiently fine-grained. Fourth, there was no assessment of social and emotional behaviors. To address these limitations, we expanded the range of the GMFCS, MACS, and EDACS and added additional, similarly configured assessments.

The in-house assessment battery evaluated ten dimensions of behavior using Likert-type (1–5 rating scale, low-normal function) questions and two dimensions using binary-response (No = 1/Yes = 5) questions, for a total of 12 behavioral categories. The Likert-type instruments were Gross Motor Function, Fine Motor Function, Eating and Drinking Ability, Tactile Perception, Visual/Visuomotor Function, Auditory Function, Receptive Language Function, Expressive Language Function, Overall Communication, and Social-Emotional Responsiveness. The first three were modifications of the GMFCS, MACS, and EDACS, respectively. The three language-assessment instruments were modeled on the CFCS. The three perceptual and the social-emotional instruments were new but were similarly constructed. The two binary-response instruments assessed Expression of Pleasure/Displeasure and Anticipation of Future.

Assessment forms were distributed to families after successful completion of the image acquisition sessions and prior to the release of any imaging results. Parents were instructed to score their child's functional abilities based on empirical observations and perceptions. Where an adequate response could not be identified, explanations and notes were encouraged. Upon receipt of the completed behavioral assessment forms, structured interviews were performed with each family either by videoconference or in-person, to review the scores, ensure scoring was consistently applied across families, and to collect detailed information about their child's functional status. The outline of the interview followed the assessment form and reviewed the functional deficits of each child, requesting specific examples of behaviors that informed the scoring. Three members of our team (MI, PTF, and MDW) participated in each interview, which were recorded and transcribed. The complete behavioral assessment battery, per-patient clinical summaries, and per-patient behavioral scores are provided in Supporting Information.

Image Acquisition

Participants were brought to the imaging suite by their parent(s) at or after their typical bedtime, typically around 8:00–9:00 p.m. Children were mildly sleep deprived by limiting daytime naps. All participants received 5 mg/kg of diphenhydramine HCl 12.5 mg/5 mL oral solution to aid in sleep induction. The children were put to bed by their parent(s) in a child-friendly bedroom adjacent to the MRI suite. When judged by the parent(s) to be deeply asleep, they were carried to the MRI suite and prepared for imaging. Preparations included placement of noise-reduction earplugs, foam head restraints, and blankets. Extra padding and sheets had already been added to the MRI table to increase comfort through the sleep scanning sequence.

T1-weighted, diffusion-weighted, and functional (BOLD) MR data were obtained in a single scanning session when possible. If all sequences could not be obtained in one night, the subject returned for repeat scanning (2 patients were rescanned). We previously reported analyses of the T1-weighted [Ishaque et al., 2016] and diffusion-weighted [Ishaque et al., 2017] data from these sessions. This study reports the rs-fMRI data.

MRI data were obtained on a 3 T Siemens TIM-Trio (Siemens Medical Solutions, Erlangen, Germany), using a standard 12-channel head coil as the RF receiver and the integrated circularly polarized body coil as the RF transmitter. T1-weighted images were acquired using the MPRAGE pulse sequence with TR/TE = 2200/2.72 ms, flip angle = 13°, TI = 766 ms, and volumes = 208, 0.8 mm isotropic voxel size. Functional (BOLD; T2*-weighted) imaging used a gradient-echo, echo-planar sequence, acquiring 29 slices, with TR/TE = 3,000/30 ms, flip angle = 90°, 2 × 2 × 4 mm spatial resolution, FOV = 200 mm, and acquisition time = 30 min.

Acquired images were visually inspected per subject for artifacts, nonrelated pathology, and/or evidence of motion. No images showed gross pathology other than variable degrees of atrophy. Three ABI and two control subject datasets demonstrated gross signs of excessive motion. These were preprocessed with FSL's MCFLIRT to determine absolute displacement parameters and were found to be beyond acceptable limits (>2 mm) in the first instance (3.27, 3.59, 3.98, 4.47, and 8.16 mm, respectively). These datasets were excluded from further consideration. Two of the ABI subjects were successfully rescanned, ultimately yielding high-quality datasets in 10 ABI and 9 control participants.

Image Preprocessing

Independent intrinsic connectivity networks were computed using the FSL (FMRIB Software Library, www.fmrib.ox.ac.uk/fsl) MELODIC software package, as follows [Beckmann and Smith, 2004]. T1-weighted anatomical images were preprocessed using the brain extraction tool (BET) to remove skull and nonbrain tissues [Smith, 2002]. FSL's MELODIC was run on the T2*-weighted BOLD images using a high-pass filter of 100 s. MCFLIRT motion correction, brain extraction, and spatial smoothing of

5 mm FWHM were applied [Jenkinson et al., 2002]. Single-session ICA with fixed dimensionality of 20 components was implemented on each subject's resting-state data. Manual denoising was performed per subject (images were thresholded at $z > 2.3$) using FSL's *fsl_regfilt* tool with the following noise component criteria: ring patterns, large activation areas across white matter/grey matter boundaries, checkerboarding, predominant posterior sagittal sinus signal, saw tooth patterns or large spikes in component time-series, and >50% of component time-series power spectrum at frequencies >1 Hz [Kelly et al., 2010]. This was an "aggressive" filtering, removing all aspects of the components identified as bad, not simply those orthogonal to good components. Global signal regression was not performed: because the technique is controversial, because "GSR should be used with care when comparing groups with different noise characteristics or varying neural network structures" [Murphy and Fox, 2017], because GSR has not been shown to improve spatial ICA network segregation, and because the FSL development team does not recommend its use. Prior to motion correction the absolution motion in the ABI group was 0.192 ± 0.070 mm and in the control group was 0.188 ± 0.83 mm. These were not significantly different ($P = 0.907$). Following motion correction, the absolute motion in the ABI group was 0.026 ± 0.011 mm and in the control group was 0.018 ± 0.13 mm. These were not significantly different ($P = 0.156$). Following motion correction, the averages of mean absolute displacement and mean relative displacement for all subjects (i.e., patients and controls) were found to be 0.022 and 0.021 mm, respectively. At the individual level, all subjects had mean absolute and relative displacement values ≤ 0.050 mm.

Between-Group Image Analysis

Multisession temporal concatenation ICA with a fixed dimensionality of 20 components was implemented on all subjects' denoised data to yield group-average ICNs [Beckmann et al., 2005]. T2* BOLD images were registered to anatomical images with a normal search and 6 degrees of freedom. Registered brains were linearly converted into standard Talairach space (full affine registration; 12 degrees of freedom) using a resampling resolution of 2 mm, with registration to the Colin27 brain template (normalized to Talairach space). Accurate registration was visually verified for all subjects, and the Colin27 template was found to be appropriate across the cohort's age range. Thresholded ICNs ($z > 3$) were identified and behaviorally interpreted by reference to the 10 resting-state networks (Cerebellum, Sensorimotor, Visual 1, Visual 2, Visual 3, Auditory, Left Frontoparietal, Right Frontoparietal, Default Mode, and Executive Function) extracted with ICA of resting-state data and the BrainMap database, as described by Smith et al. [2009] (i.e., by referencing the functional attributions they made to these ICNs). The basal ganglia network was additionally identified and interpreted [Robinson et al., 2009]. Only the 11 components of interest were retained for further analysis.

The refined set of spatial maps from the group-average analysis was used to generate subject-specific spatial maps and associated time series using dual regression in FSL [Beckmann et al., 2009; Filippini et al., 2009]. For each subject, the group-average set of spatial maps was regressed (as spatial regressors in a multiple regression) into the subject's 4D space-time dataset. This resulted in a set of subject-specific time series, one per group-level spatial map. Those time series were regressed (as temporal regressors, again in a multiple regression) into the same 4D dataset, resulting in a set of subject-specific spatial maps, one per group-level spatial map. We tested for group differences per network using FSL's *randomise* permutation-testing tool (5,000 permutations) and Bonferroni-corrected for multiple comparisons (for 11 networks and a two-tailed t test).

Within-Patient-Group Image Analysis

For per-subject, within-patient-group analysis, study-specific network templates were established from the group ICA of control subjects' data ($z > 2.3$) (Fig. 5). These network component templates served as the standard for identification and comparison of each subject's individual ICA decomposition. Included networks reflect the 10 ICNs described by Smith et al. [2009] and the basal ganglia network.

Network preservation was investigated through network absence/presence and network volume measures. In measuring network preservation, we assess the extent to which the ICNs are intact, or uninjured. Network absence/presence was noted through visual inspection of the overlap of individual component maps with network templates. Network identification was then validated by spatial cross-correlation of single-subject networks with the control-group derived network templates following the methods described by Smith et al. [2009]. This automated labeling technique did not change any component identifications. The paired networks had a mean Pearson's $r = 0.43$ (0.20:0.73).

Total network volumes and percent overlap of each network with the corresponding template network were calculated per subject using Mango tools (www.ric.uthscsa.edu/mango/). Total network volume was calculated as follows: (1) a single component was loaded onto the standard Talairach brain, (2) the *Threshold to ROI* function was used to create an ROI around the component, (3) creation of an accurate ROI was confirmed by visual inspection, and (4) volume in voxels was calculated within the ROI using the *ROI Statistics → Volume* functions. Network percent overlap was calculated as follows: (1) the two components of interest were loaded onto a single standard Talairach brain (e.g., single-patient Auditory network and

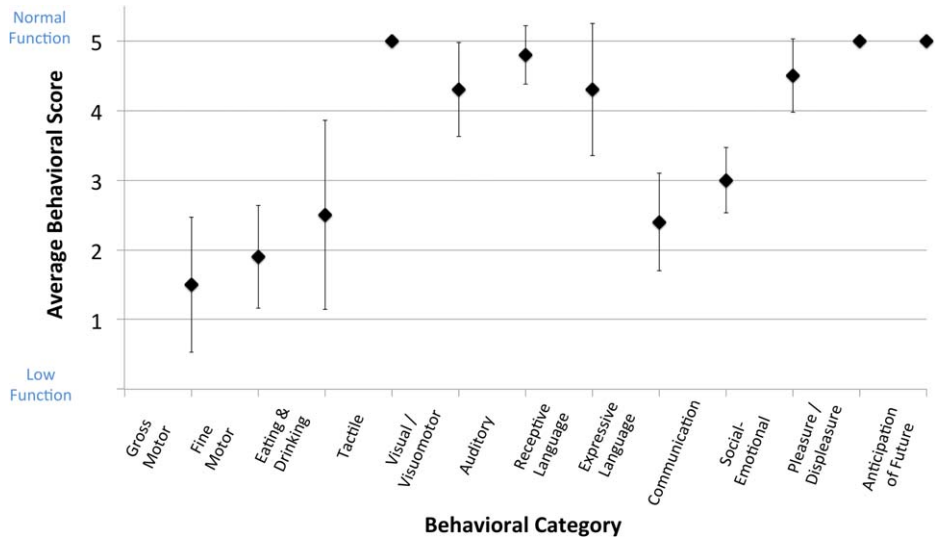

Figure 1.

Average ABI behavioral data. Average behavioral scores and standard deviations for anoxic brain injury (ABI) patients are shown for 12 behavioral categories. The first 10 categories were assessed with a 1–5 scoring system (low–normal function); the last 2 categories were assessed with a Yes/No response (Yes = 5, No = 1). See Supporting Information for complete behavioral assessment form contents. Note: all control subjects were scored at a 5 for all behavioral categories.

template Auditory network), (2) the *Create Overlay Logicals* tool was used to show areas of overlap between the two component images, (3) the volume in voxels of the overlapping region(s) was calculated using the *Create stats of this region* tool from within the Logicals interface, and (4) this volume was divided by the total network volume of the template network to determine a percentage of overlap (e.g., (overlap volume of Auditory networks/volume of template Auditory network) × 100) in Microsoft Excel. These imaging metrics characterized the relative extent and spatial position of the identified ICNs, and they were further utilized in correlation analyses.

Imaging–Behavioral Correlation

Correlation between per-subject imaging metrics (Network Percent Overlap) and behavioral scores (as described above) in ABI patients was assessed after subclassifying ICNs and behavioral categories into three subgroups: Motor, Sensory, and Cognition. The Motor network grouping was composed of the Basal Ganglia and Cerebellar networks; the Motor behavioral grouping included the Gross Motor Function, Fine Motor Function, Eating & Drinking Ability, and Expressive Language Function categories. The Sensory network grouping was composed of the Sensorimotor, Visual 1, Visual 2, Visual 3, and Auditory networks; the Sensory behavioral grouping included the Tactile Perception, Visual/Visuomotor Function, and Auditory Function categories. The Cognition network grouping was composed of the Left Frontoparietal, Right Frontoparietal, Default Mode, and Executive Function networks; the Cognition behavioral grouping included Receptive Language Function, Overall Communication, Social-Emotional Responsiveness, Expression of Pleasure/Displeasure, and Anticipation of the Future categories. Network Percent Overlap values and behavioral scores were averaged within the described groupings to provide a Motor, Sensory, and Cognition network preservation value and a Motor, Sensory, and Cognition behavioral value per patient (3 behavioral scores and 3 network values per patient). The R statistical environment (R Core Team 2017) and lme4 [Bates et al., 2015] were used to perform a linear mixed-effects model analysis of the relationship between network percent overlap and behavioral scores. The mixed-effect model controlled for the variance associated with multiple measures from the same subject. In computing Spearman's rank correlation, the network preservation and behavioral scores within-subject were modeled as a fixed effect, and the random intercepts which are allowed to vary between subjects were modeled as a random effect.

RESULTS

Group-Level Analysis

Behavioral assessment

Average behavioral scores for the ABI patients were 0.50 (±0.97) for Gross Motor Function; 1.90 (±0.74) for Fine Motor Function; 2.50 (±1.35) for Eating and Drinking

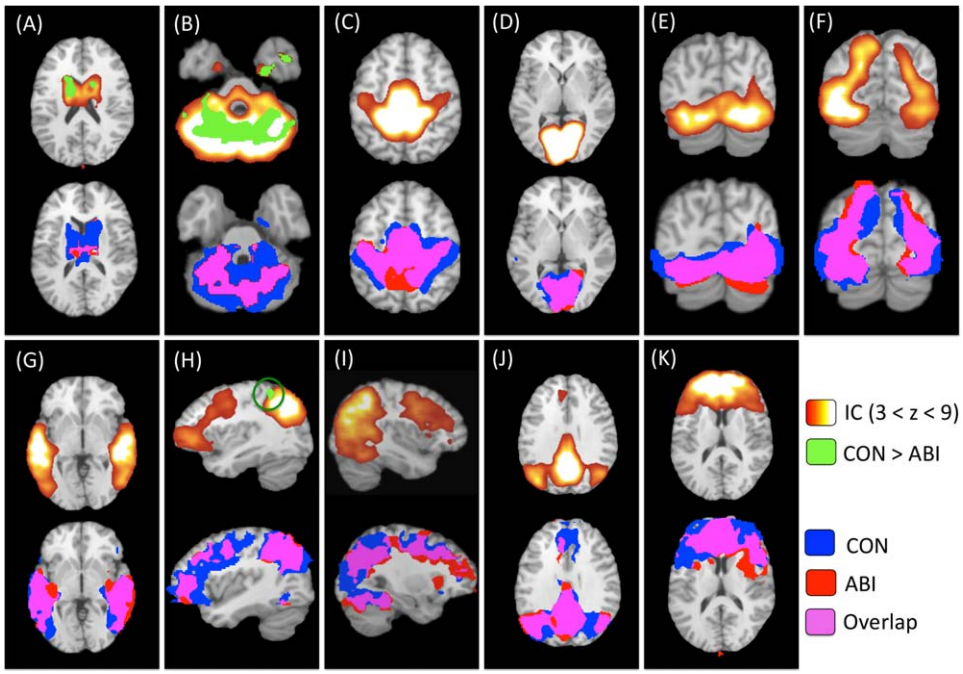

Figure 2.

Group independent components analysis and dual-regression results. *Top row*: The 11 intrinsic connectivity networks (ICNs) of interest resulting from independent components analysis (ICA) of all subjects' data are shown on the top row of panels (A)–(K) in red–yellow–white. The identified ICNs are classified as follows: (A) basal ganglia; (B) cerebellum; (C) sensorimotor; (D) Visual 1; (E) Visual 2; (F) Visual 3; (G) auditory; (H) left frontoparietal; (I) right frontoparietal; (J) default mode; and (K) executive function. These ICNs were used to compute group contrasts and group-specific maps per network. Between-group differences (controls > patients) are overlaid onto the original ICN maps (*top row*) in green ($P < 0.05$, corrected for multiple comparisons). *NB*: significant between-group differences were observed in three ICNs: (A) basal ganglia, (B) cerebellum, and (H) left frontoparietal. *Bottom row*: Group-specific maps for each ICN are shown on the bottom row of each panel. Control group-specific networks are displayed in blue; patient group-specific networks are displayed in red; overlap between control and patient group networks is displayed in pink ($P < 0.05$). All images are overlaid onto the Talairach standard brain. IC, independent component; CON, control; ABI, anoxic brain injury.

Ability; 5.00 (±0) for Tactile Perception; 4.30 (±0.67) for Visual/Visuomotor Function; 4.80 (±0.42) for Auditory Function; 4.30 (± 0.95) for Receptive Language Function; 2.40 (±0.70) for Expressive Language Function; 3.00 (±0.47) for Overall Communication; 4.50 (±0.53) for Social-Emotional Responsiveness; 5.00 (±0) for Expression of Pleasure/Displeasure; and, 5.00 (±0) for Anticipation of the Future (Fig. 1). The lowest average scores thus involved motor functions (i.e., gross and fine motor function, eating and drinking, and expressive language). Other sensory and higher order functions were found to be relatively behaviorally intact across the patient group. All control subjects were scored at a 5.00 for all categories, thus representing normal functioning.

Network analysis

We were able to identify and isolate all 11 networks of interest (Basal Ganglia, Cerebellum, Sensorimotor, Visual 1, Visual 2, Visual 3, Auditory, Left Frontoparietal, Right Frontoparietal, Default Mode, and Executive Function) from the initial ICA analysis implemented on all subjects' resting-state fMRI data (Fig. 2, *top row*).

Regression of these ICNs to group-specific maps demonstrated substantial preservation of the Sensorimotor, Visual 1–3, Auditory, and Default Mode networks in the patient group. Less preservation was observed in the Left Frontoparietal, Right Frontoparietal, and Executive Function networks. The least preservation was observed in the Basal Ganglia and Cerebellar networks ($P < 0.05$; Fig. 2, *bottom row* and Fig. 3).

Significant between-group differences were measured in the Basal Ganglia, Cerebellar, and Left Frontoparietal networks ($P < 0.05$, corrected; Fig. 2, *top row* and Table II). Peak areas of decreased ICN connectivity in the ABI patient group were identified in bilateral caudate bodies (Basal Ganglia), posterior cerebellar lobe (Cerebellum), and left inferior parietal lobule (Left Frontoparietal). No

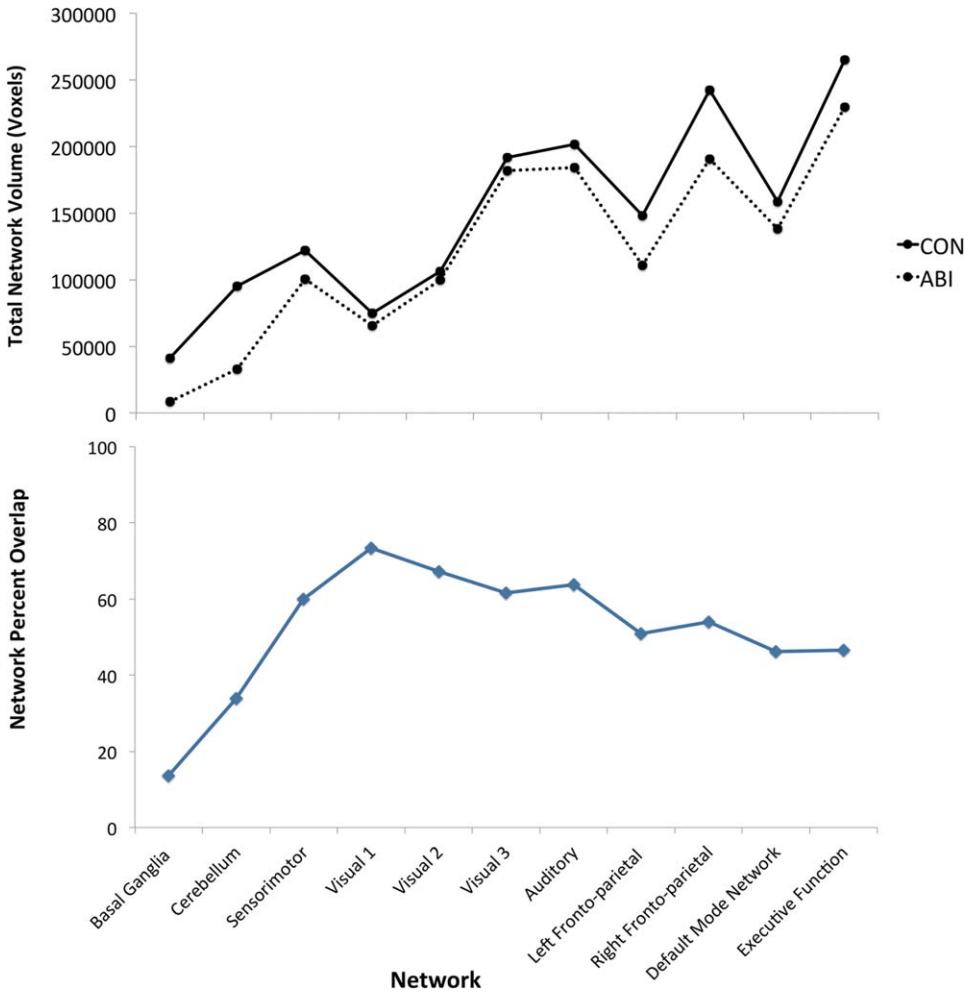

Figure 3.

Top: The total volume (in voxels) of each group-specific intrinsic connectivity network (ICN) is shown for patient and control groups. *Bottom*: The percent overlap of each patient-group ICN with the corresponding control-group ICN is shown. CON, control; ABI, anoxic brain injury.

significant areas of increased network connectivity were observed in the patient group relative to the control group (Table II).

Subject-Level Analysis

Behavioral assessment

As reported above for average behavioral scores, ABI patients were found to overall have low motor function (Gross Motor, Fine Motor, Eating and Drinking, Expressive Language) and relatively higher emotive/cognitive (Receptive Language, Overall Communication, Social-Emotional, Expression of Pleasure/Displeasure, Anticipation of the Future) and sensory perception (Tactile, Visual/Visuomotor, Auditory) function (Fig. 4). The greatest variation in behavioral function was measured in Eating and Drinking Ability; there was no variation in the Tactile Perception, Expression of Pleasure/Displeasure, or Anticipation of Future categories.

Network analysis

Using the group-wise ICNs from control subjects as per-network normal templates (Fig. 5), per-subject ICNs were extracted and quantified for both groups. Figure 6 demonstrates the range of network preservation (absent/low, moderate, and high) for each ICN (by total volume) among ABI patients. In terms of absence/presence of ICNs, the cerebellar network was most frequently absent (5 times). The left frontoparietal network had the second highest frequency of absence (2 times), and the Basal Ganglia, Visual 1, Right Frontoparietal, and Executive Function networks were each unidentified once (Fig. 7, *top*).

TABLE II. Between-group network differences

Anatomical location	Hemisphere	Talairach coordinates of global maxima			Extent (voxels)
		x	*y*	*z*	
Control > ABI					
Basal ganglia					
Caudate body	L	−14	1	19	3,885
Caudate body	R	15	2	12	1,273
Cerebellum					
Posterior lobe	L	−27	−71	−24	37,901
Left frontoparietal					
Inferior parietal lobule	L	−36	−46	54	2,503

Locations, coordinates, and extents of peaks of significant between-group differences in intrinsic connectivity network (ICN) connectivity (from group ICA and dual regression analysis) are shown. Significant differences were identified in three ICNs: basal ganglia, cerebellum, and left frontoparietal (Controls > Patients; $P < 0.05$, corrected for multiple comparisons).

Among the identified ICNs in ABI patients, relative preservation of the Sensorimotor, Visual 1–3, Auditory, and Default Mode networks was observed. Less preservation was seen in the Left Frontoparietal, Right Frontoparietal, and Executive Function networks. The least preservation was observed in the Basal Ganglia and Cerebellar networks (Fig. 7, *middle and bottom*). The largest per-patient variation in network volume was measured in the Left Frontoparietal, Right Frontoparietal, and Executive Function networks, and the smallest variation was measured in the Sensorimotor, Visual 2, and Basal Ganglia networks (in order).

Imaging–Behavioral Correlation

Per-patient network percent overlap values and behavioral scores were subgrouped into Motor, Sensory, and Cognition categories, and an overall positive correlation was measured between the image and behavioral metrics. Spearman's correlation coefficient was $\rho = 0.74$ ($P = 0.0001$, 95% confidence interval = 0.51–0.87) (Fig. 8). Clear separation of values from the Motor, Sensory, and Cognition subgroups was observed. A low to high trend in network preservation percentages and behavioral scores was discernible with motor, cognition, and perceptual values (in that order).

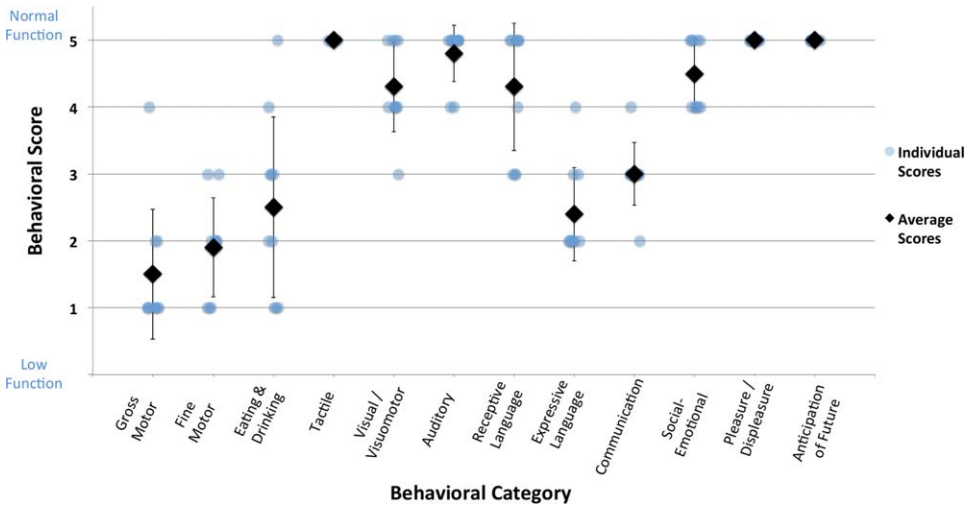

Figure 4.

Per-subject ABI behavioral data. Per-subject behavioral scores (with averages and standard deviations) for ABI patients are shown for 12 behavioral categories. The first 10 categories were assessed with a 1–5 scoring system (low–normal function); the last 2 categories were assessed with a Yes/No response (Yes = 5, No = 1). See Supporting Information for complete behavioral assessment form contents.

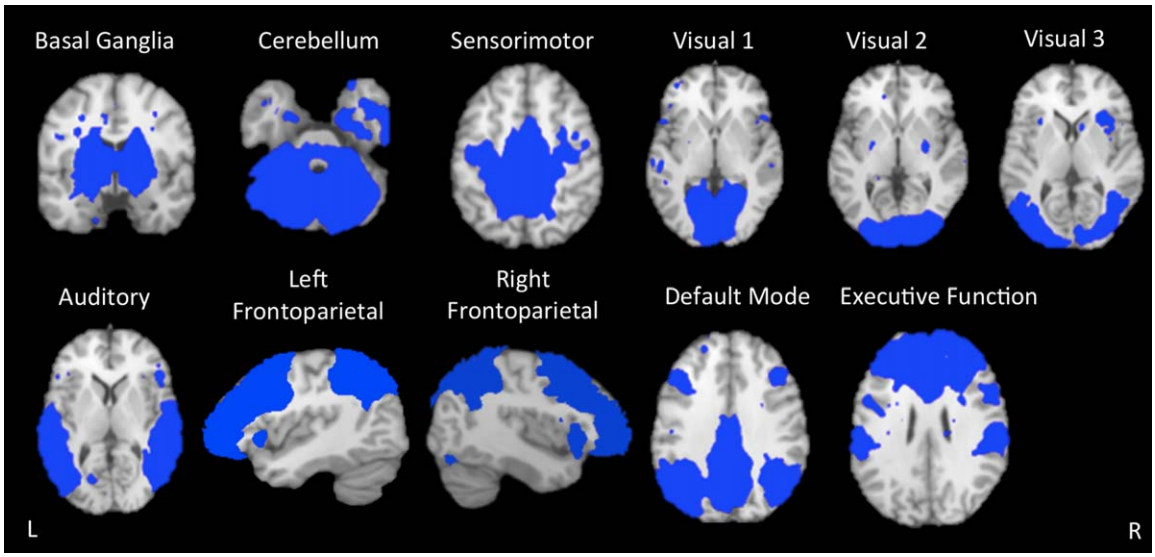

Figure 5.

Intrinsic connectivity network templates. Study-specific templates of 11 intrinsic connectivity networks (ICNs) extracted from independent components analysis of controls subjects' resting-state fMRI data are shown. The included networks reflect the 10 standard ICNs, as described by Smith et al. [2009], plus the basal ganglia network. Networks are overlaid onto the Talairach standard brain.

DISCUSSION

We acquired long-duration rs-fMRI data in children with drowning-induced ABI and neurotypical controls using a nocturnal, drug-aided sleep fMRI protocol. Network integrity was quantified by independent components analysis (ICA), at both group- and per-subject levels. Quantitative behavioral assessments designed to correspond to canonical, ICA-derived networks were obtained from parents and caregivers via structured interviews. Motor ICNs (Basal Ganglia, Cerebellum) were grossly compromised in ABI patients both group-wise and individually, concordant with their prominent motor deficits. Striking preservations of perceptual (Visual, Auditory, Sensorimotor) and cognitive ICNs (Default Mode, Frontoparietal, Executive Function) were observed, and the degree of network preservation correlated ($\rho = 0.74$) with per-subject functional status assessments. Our hypotheses were validated as (1) rs-fMRI demonstrated group-level differences between patients and controls, (2) per-patient abnormalities were successfully and meaningfully elicited, (3) imaging and behavioral results demonstrated concordance, and (4) motor-network abnormalities were much more severe than perceptual- and cognitive-network abnormalities. Collectively, our findings indicate that the severe motor deficits observed in this population can mask relatively intact perceptual and cognitive capabilities.

The 11 ICNs of interest (Basal Ganglia, Cerebellum, Sensorimotor, Visual 1, Visual 2, Visual 3, Auditory, Left Frontoparietal, Right Frontoparietal, Default Mode, and Executive Function) were distinguishable at group and individual subject levels with ICA. In both group-wise and per-patient network analyses, greatest network preservation was observed in the Sensorimotor, Visual 1, Visual 2, Visual 3, Auditory, and Default Mode networks. Less preservation was observed in the Left Frontoparietal, Right Frontoparietal, and Executive Function networks. The least preservation was observed in the Basal Ganglia and Cerebellar networks. Compared to the control group, patients with ABI showed decreased functional connectivity in the Basal Ganglia, Cerebellar, and Left Frontoparietal networks. The Cerebellar network was most frequently absent (i.e., undetectable) in individual patients.

Behavioral assessments demonstrated that children with ABI had relatively intact function on the Tactile Perception, Visual/Visuomotor Function, Auditory Function, Receptive Language Function, Overall Communication, Social-Emotional Responsiveness, Expression of Pleasure/Displeasure, and Anticipation of Future instrument. Less behavioral integrity was observed in the Gross Motor Function, Fine Motor Function, Eating and Drinking Ability, and Expressive Language Function categories. Per-subject image metrics and behavioral scores overall correlated strongly. Furthermore, Motor, Cognitive, and Sensory subgroups separated out quite well (in order of increasing preservation) along the network and behavioral preservation scale. High concordance was thus observed in the evaluation of functional integrity by intrinsic connectivity network preservation and behavioral assessments, at both group and per-subject levels.

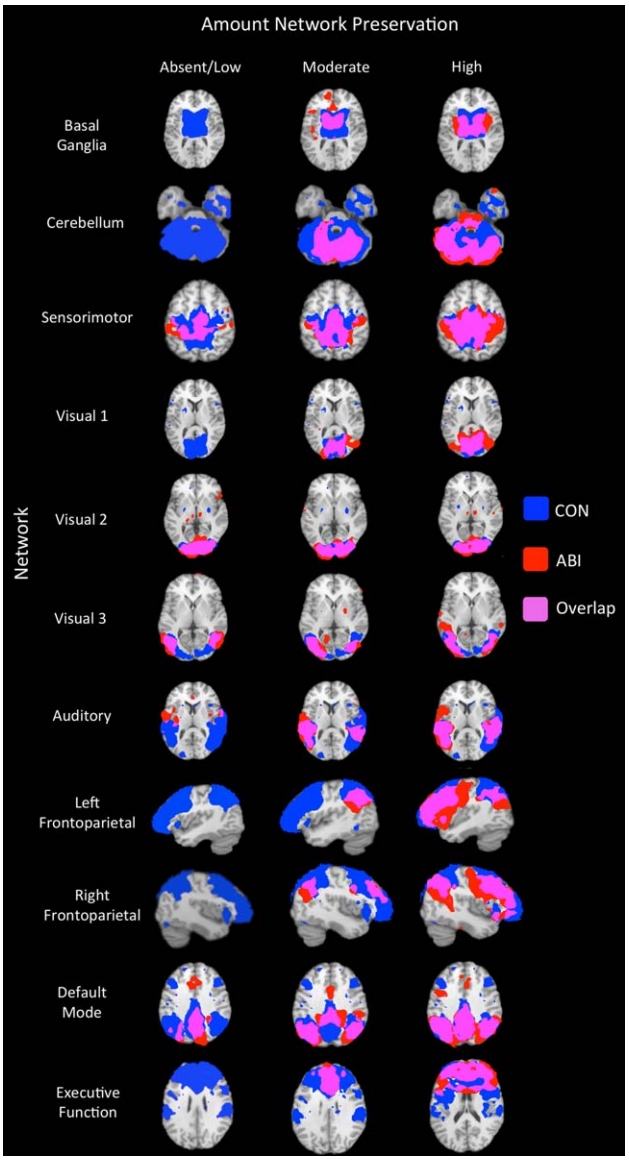

Figure 6.

ABI per-subject network preservation. The range of intrinsic connectivity network (ICN) preservation among individual anoxic brain injury (ABI) patients is shown for the 11 ICNs of interest. Each row illustrates the range of network preservation observed across ABI patients within a single network. Each column illustrates the least preservation (left column), typical preservation (middle column), and most preservation (right column) across all subjects. Note, no single row or column represents an individual subject. ICN templates derived from the control-group independent components analysis (Fig. 5) are displayed in blue; individual patient networks are displayed in red; overlap between the template and patient networks is displayed in pink ($z > 2.3$). Absent/low, moderate, and high levels of network preservation are depicted based on network volume. All images are overlaid onto the Talairach standard brain. CON, control; ABI, anoxic brain injury.

In all analyses, pathology was largely limited to the motor system (i.e., Basal Ganglia and Cerebellar networks; Gross Motor Function, Fine Motor Function, Eating and Drinking Ability, and Expressive Language Function behavioral categories). Striking relative preservation of sensory (i.e., Sensorimotor, Visual 1–3, and Auditory networks; Tactile Perception, Visual/Visuomotor Function, and Auditory Function behavioral instruments) and higher cognitive (i.e., Default Mode network; Receptive Language Function, Overall Communication, Social-Emotional Responsiveness, Expression of Pleasure/Displeasure, and Anticipation of Future behavioral instruments) functions was evident.

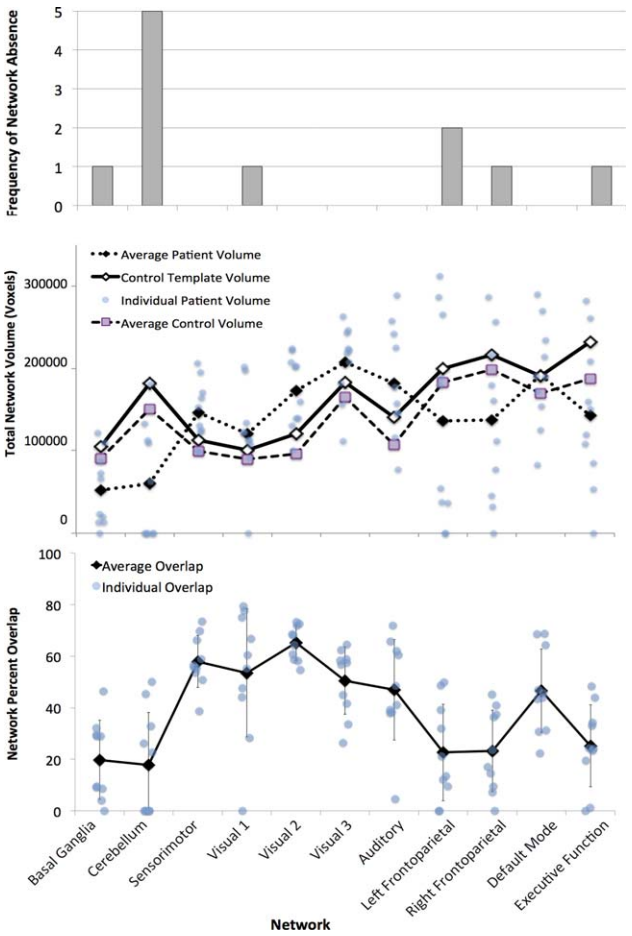

Figure 7.

Top: The frequency of network absence in individual patients' independent components analyses (ICA) is shown per intrinsic connectivity network (ICN). *Middle*: The total volume in voxels of each ICN is shown for individual patients. Total volume means for each ICN are shown for individual patient and control volumes. The volumes of ICN templates derived from the control group's ICA are also displayed. *Bottom*: The percent overlap of each patient's ICN with the corresponding template ICN is shown, along with means and standard deviations.

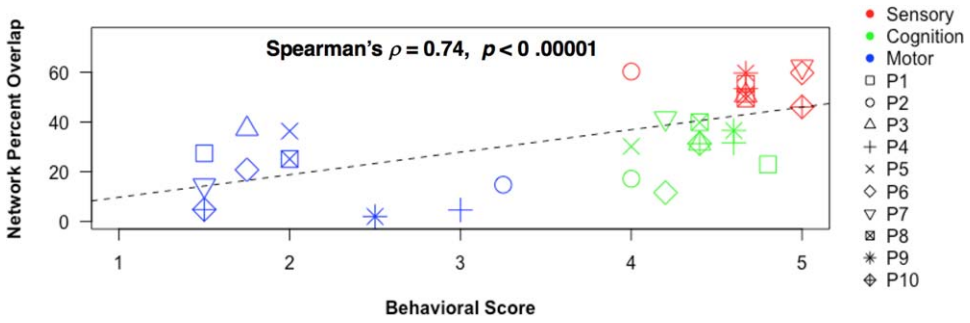

Figure 8.

Imaging–behavioral correlation. Individual patients' network percent overlap values (with the corresponding network templates) are shown plotted against individual patients' behavioral scores, both averaged within motor, sensory, and cognition subgroups. Each symbol represents an individual patient (P1–P10), with 3 behavioral values and 3 network-preservation values per patient. *Motor* = Basal Ganglia and Cerebellar networks; Gross Motor Function, Fine Motor Function, Eating & Drinking Ability, and Expressive Language Function behavioral categories. *Sensory* = Sensorimotor, Visual 1, Visual 2, Visual 3, and Auditory networks; Tactile Perception, Visual/Visuomotor Function, and Auditory Function behavioral categories. *Cognition* = Left Frontoparietal, Right Frontoparietal, Default Mode, and Executive Function networks; Receptive Language Function, Overall Communication, Social-Emotional Responsiveness, Expression of Pleasure/Displeasure, and Anticipation of the Future behavioral categories.

Taken together, this pattern of functional impairment/integrity builds upon our previous structural grey and white matter analyses demonstrating predominant motor-system damage to suggest that children with drowning-related ABI can suffer from a deefferentation syndrome with relative preservation of perceptual and cognitive abilities. Structural and functional motor deficits appear to preclude outward expression of relatively intact perceptual, cognitive, and emotional abilities. Indications of this level of functional integrity were detected behaviorally, but only through a novel, caregiver-driven behavioral assessment strategy designed for this population. The discussion below will expand on the correlates of these impactful findings. Additionally, further examination of the potential clinical impact of our imaging protocol in per-subject assessment and prognostication is warranted.

Group-Level Image Analysis

Significant decreases in functional connectivity in the ABI patient group were measured in the Basal Ganglia, Cerebellar, and Left Frontoparietal networks. Peak decreased connectivity within the Basal Ganglia network localized to bilateral caudate bodies. The basal ganglia consist of subcortical nuclei involved in motor, associative, and limbic circuits. Their role in voluntary motor activity, control, and coordination is well established, and the Basal Ganglia intrinsic connectivity network has been shown to be altered in several movement disorders [Laird et al. 2011; Luo et al., 2012; Robinson et al., 2009; Szewczyk-Krolikowski et al., 2014]. Functional compromise of this network likely underlies the substantial motor deficits routinely reported in this population. Injury may extend to the associative and limbic functions of the basal ganglia as well.

A large region of decreased functional connectivity was identified in the Cerebellar network, with a maximum in the posterior lobe. The cerebellum is implicated in several functions, but the most prevalent descriptions of this network involve action execution and motor coordination [Laird et al., 2011; Smith et al., 2009]. Functional compromise of the Cerebellar network likely contributes to substantial motor impairments observed in the patient group. Interestingly, prominent structural damage to the cerebellum was not observed in our VBM analysis [Ishaque et al., 2016].

Finally, a small region of hypoconnectivity in the Left Frontoparietal network, with a peak in the left inferior parietal lobule was identified. The Left Frontoparietal network is strongly implicated in language comprehension and production [Laird et al., 2011; Rosazza and Minati, 2011; Smith et al., 2009]. Functional compromise of the left frontoparietal network likely contributes to the expressive language deficits observed in the patient group.

Aside from these regions of decreased functional connectivity, no significant between-group differences were identified in the Sensorimotor, Visual 1–3, Auditory, Right Frontoparietal, Default Mode, or Executive Function networks. This suggests relatively intact sensory and higher cognitive function in the patient group. This pattern of preservation was seen in the behavioral data as well, with motor-system behavioral functions being most affected (1.50, 1.90, 2.50, and 2.40 average scores for Gross Motor, Fine Motor, Eating and Drinking, and Expressive Language functions, respectively).

Subject-Level Image Analysis

Long scan duration (30 min) enabled the application of ICA to individual-patient data, mediating meaningful per-

subject, per-network interpretation. This is promising when considering the potential clinical impact of these methods.

The greatest compromise in functional connectivity was seen in the motor resting-state networks (i.e., Cerebellum and Basal Ganglia) across ABI patients. The Cerebellar network was undetectable in 5/10 patients (17.8% average preservation). In some MRI acquisitions, the cerebellum is not fully covered in the scan due to a limited field of view (FOV) [Smith et al., 2009]. Limited FOV cannot explain our observation as we confirmed both at acquisition and prior to processing that the cerebellum was within the FOV. Furthermore, the Cerebellar ICN was detected in all control subjects, and between-group functional connectivity differences were also observed in the group-level analysis. Thus, as suggested above, functional compromise of the Cerebellar network likely contributes to the observed motor deficits in this population. The extent of cerebellar impairment is nevertheless quite striking in comparison to our VBM structural findings, in which a relatively small region of atrophy was identified in the posterior lobe [Ishaque et al., 2016]. Cerebellar dysfunction may arise, at least in part, due to functional deafferentation following the predominant subcortical injury to the basal ganglia and PLICs. Cerebellar diaschisis, first reported by Baron et al. [1981] has been described to manifest as reduced metabolism and blood flow in the cerebellum following, and contralateral to, a supratentorial lesion. Interruption of excitatory cortico-ponto-cerebellar pathways—including PLIC lesions—is thought to be the underlying mechanism of cerebellar dysfunction [Carrera and Tononi, 2014]. Functional disconnection of the cerebellum may thus be a downstream effect of the primary central subcortical insult. This would be consistent with the absence of substantial cerebellar atrophy in the group-wise morphometric analysis, in which the strongest and most consistent structural differences are measured. Cerebellar ischemia could be further investigated using perfusion weighted imaging methods [Petrella and Provenzale, 2012].

The Basal Ganglia network was undetected in one patient. In patients where it was detected, it showed great impairment as measured by total volume and percent overlap with the normal template (19.8% average preservation). Again, this likely drives the resultant motor dysfunction.

Sensory networks (i.e., Sensorimotor, Visual 1–3, and Auditory) were notably found to be intact per patient (58.0%, 56.3% (Visual 1–3 average), and 47.0% average preservation, respectively), suggesting preserved tactile, visual, and auditory processing in ABI children. The Default Mode network was also largely intact per patient (detected in 10/10 patients, 46.6% average preservation), suggesting preserved introspective processes, self-awareness, and social cognition (self vs other awareness) [Broyd et al. 2009; Rosazza and Minati, 2011; Smith et al. 2009]; this point will be expanded upon below. Other higher order networks (i.e., Left Frontoparietal, Right Frontoparietal, and Executive Function) were more variable in their preservation (22.6%, 23.2%, and 25.2% average preservation, respectively). Nevertheless, striking preservation of these ICNs was indeed discovered in some patients (Figs. 6 and 7). Complex functions including language comprehension, working memory, spatial awareness, attention allocation, perception of the future, and cognitive control may well be conserved to a level previously unsuspected in this population [Beckmann et al. 2005; Laird et al. 2011; Rosazza and Minati, 2011; Smith et al. 2009]. Functional connectivity findings overall corresponded well with per-subject behavioral scores, conveying low motor function and relatively high perceptual and cognitive function. The observed integrity of higher order networks may in part stem from the typical timeline of cerebral network development and integration. Neural regions serving more "elementary" motor and sensory functions are thought to mature earlier than those involved in complex, higher-order cognitive processes [de Bie et al. 2012]. Given the average age of accidental drowning, both within our cohort (2.4 year-average) and in the population-at-large (1–4 years), it is possible the relative sparing of cognitive networks results from their comparative immaturity at the time of the anoxic insult. That is, motor networks may sustain greater damage in pediatric drowning than other systems that are less developed in young children.

Imaging–Behavioral Correlation

The caregiver-based, quantitative behavioral assessment strategy—using structured interviews to assess behavior comprehensively and in a network-based manner—worked well. Behavioral and image-derived metrics of network integrity were mutually predictive at a highly significant level ($\rho = 0.74$; $P < 0.0001$). The behavioral validity of the imaging results is thus plausible. Furthermore, a clear trend in network preservation and behavioral integrity was visible among the Motor, Sensory, and Cognition subgroups. Motor-system impairment was discernible through the lowest network preservation and behavioral function in the Motor subgroup. This mirrored the compromised gross and fine motor function, eating and drinking abilities, and the ability to produce speech. Sensory perception was shown to be relatively intact with the highest network preservation and behavioral function in the Sensory subgroup. This mirrored the relatively preserved abilities to perceive tactile, visual, and auditory stimuli. Similarly, higher order cognitive functions were shown to be moderately intact, with intermediate network preservation and behavioral scores. These trends support the overall group-wise and per-subject conclusions derived from imaging and behavioral data. We believe implementation of the same analyses in a larger cohort would provide additional support for the observed imaging–behavioral correlation.

Compensatory Neural Mechanisms

In group- and subject-level analyses, prominent expansion in certain networks was detected in patients relative to controls (see red regions in Fig. 6). Network volume averages in individual patients approximated or exceeded those of the corresponding control templates in the Sensorimotor, Visual 1, Visual 2, Visual 3, Auditory, and Default Mode networks. Networks with greater overall preservation at both group- and individual-level analyses were thus also found to have notable expansion in connected volume. Although subject variability and registration effects may explain this to some extent, the observation suggests that neural plasticity is being exhibited. Less damaged networks will experience preferential use, encouraging expansion. Attenuation of inhibitory input from damaged networks and pathways (disinhibition) could also contribute to the observed expansion [Merzenich et al., 2014]. Neuroplasticity is most readily demonstrable during early postnatal years [Hensch, 2005; Merabet and Pascual-Leone, 2009; Mundkur, 2005; Rocha-Ferreira and Hristova, 2016] (although brain remodeling is now thought to be inducible at any age) [Merzenich et al., 2014]. The average age at injury in our patient cohort (2.6 ± 1.1 years) falls within this critical period, supporting this interpretation. Neuroplasticity has been implicated in recovery from several pediatric neurological disorders, including other hypoxic-ischemic etiologies [Merabet and Pascual-Leone, 2009; Mundkur, 2005; Rocha-Ferreira and Hristova, 2016], lending further credence to this hypothesis. Accordingly, expansion of perceptual and Default Mode ICNs may well reflect active (and ongoing) neuroplasticity. Monitoring ICN reorganization longitudinally following anoxic injury in this population could provide further evidence in this regard.

Significance of Default Mode Network Preservation

As reported above, the default mode network (DMN) was substantially preserved in each patient. The DMN is a highly investigated intrinsic connectivity network that corresponds to the brain's default, task-negative state [Raichle et al. 2001; Rosazza and Minati, 2011]. The DMN has been associated with higher mental processes including introspection, social cognition, motivational drive, self-referential thought, and interoception, and less-definitive concepts such as mind-wandering and day-dreaming [Heine et al. 2012; Raichle, 2015]. Dysfunction of this network has been implicated in neuropsychiatric disorders including but not limited to dementia, epilepsy, unipolar and bipolar mood disorders, autism, schizophrenia, and attention-deficit/hyperactivity disorder [Broyd et al. 2009; Rosazza and Minati, 2011]. Moreover, it has been posited as the functional basis of neural processes subserving consciousness [Vanhaudenhuyse et al. 2010]. Studies in patients with disorders of consciousness revealed decreased glucose metabolism [Laureys et al., 2004], and decreased structural and functional connectivity of the DMN in patients with decreased levels of arousal and awareness [Demertzi et al. 2014; Fernández-Espejo et al., 2012; Vanhaudenhuyse et al., 2010]. Although the diagnostic value of DMN network preservation in assessing level of consciousness in patients who cannot communicate their internal states is not yet firmly established, its preservation in our patient cohort and its correspondence with caregiver's assessment of situational awareness support the possibility of greater levels of awareness of self and others than have been previously expected or reported.

A physiological explanation for the striking preservation of the DMN, particularly relative to the other higher order cognitive networks, might be found in its high glycolytic index. The DMN has been shown to use less oxygen per mole of glucose consumed than other cortical networks [Vaishnavi et al. 2010; Vlassenko et al. 2010]. Oxygen deprivation from drowning, therefore, would likely cause less direct injury to areas with a high glycolytic index (i.e., DMN regions) relative to those with a greater dependency on oxygen.

Postdrowning Pediatric ABI as a Selective Deefferentation Syndrome

Our prior structural neuroimaging reports in this same patient cohort demonstrated grey- and white-matter loss in the lenticulostriate arterial distribution, predominately affecting motor system components (pyramidal tract and basal ganglia), with relative sparing elsewhere [Ishaque et al. 2016, 2017]. TBSS clearly demonstrated a lesion in the PLIC in which the degree of white-matter damage correlated with motor-performance impairment. The present report extends this line of investigation by applying rs-fMRI and quantitative behavioral assessments to provide functional neuroimaging and behavioral evidence of selective motor-system impairment with relative preservation of perceptual and cognitive function in children with postdrowning ABI. Collectively, these observations suggest that the substantial motor deficits in these children—all are quadriplegic and most (7/10) are aphonic—arising from structural damage to the basal ganglia and posterior limb of the internal capsule, and from functional compromise of the Basal Ganglia and Cerebellar networks, effectively prohibit full expression of their level of awareness and cognition. Task-activation fMRI [Monti et al. 2010] and rs-fMRI [Heine et al. 2012] has been successfully applied to demonstrate cognitive-system preservation in cryptic disorders of consciousness. Here, we extend this line of investigation to rs-fMRI in children with postdrowning anoxic injury.

Categorizations of cryptic disorders of consciousness and communication have evolved substantially since the initial description of LIS by Plum and Posner [1966], to include various degrees of LIS (Classical, Incomplete, and

Total) [Bauer et al., 1979]; Minimally Conscious State (MCS) and various degrees thereof (MCS+ and MCS−); and, most recently, Functional LIS [Bruno et al. 2009]. In proposing the diagnostic category Functional LIS, Bruno et al. [2009] distinguished between clinical and paraclinical testing, with paraclinical tests including EEG, evoked potentials, positron emission tomography, and functional MRI. Laureys et al. [2004] reviewed the role of imaging studies in supporting diagnosis in these disorders, placing specific emphasis on preservation of the DMN. Here, we have used network analysis of sleep-state fMRI and quantitative caregiver behavioral assessments as paraclinical tests to supplement clinical assessments and confirm that postdrowning ABI can cause a selective deefferentation syndrome ranging from Incomplete and Classical LIS to Total LIS/MCS+. All patients in our cohort met [Bruno et al., 2009] criteria for Functional LIS.

Ethical issues regarding the clinical management (e.g., acute care decisions pertaining to withdrawal of life-support) and treatment (e.g., pain and symptom control, stimulation, and overall handling) of these patients must be considered. Aside from establishing residual function, the per-subject network analysis results could inform potential avenues of communication, guide therapeutic stimulation through intact functions (e.g., reading to a child with a strong Auditory network; displaying visual stimuli when Visual networks are intact), guide targeted therapy, and monitor effects of therapeutic interventions through qualitative and quantitative network analysis. The results of the present investigation have been provided to their families and clinicians and are already impacting care in this cohort. Importantly, where metrics such as the duration of circulatory arrest and acute imaging findings fail to reliably predict outcomes, ICN profiles per patient could help clinicians with assessment and prognostication in postdrowning ABI.

Epidemiology

Postdrowning pediatric selective deefferentation may well be a common condition. The precise prevalence, however, is difficult to estimate. Data on nonfatal drownings are difficult to attain, especially in a standardized way [Topjian et al., 2012]. However, given the rates of pediatric drowning (>3,500/year in the US) and survival (>2/3 of drowning victims), there must be a large population of children that survive drowning with clinically significant ABI (> 50% of survivors require hospitalization) [Borse and Sleet, 2009; Centers for Disease Control and Prevention (CDC), 2012]. The fraction of children with postdrowning ABI suffering from an unrecognized selective deefferentation is difficult to estimate, as the syndrome was not previously recognized. In our cohort, 10/10 patients had severe impairment of motor function and relative preservation of perception and cognition, both behaviorally and by functional imaging, suggesting that this is a common condition.

We must consider, however, that our findings are likely affected by a patient-selection bias. Specifically, parents of victims were motivated to participate by their own impressions of preserved awareness and cognition in their children (although this was not an inclusion criterion). That is, their suspicion of functional preservation likely incited them to seek further support and information, and thus to learn about and participate in our study. To address these important limitations in epidemiological knowledge of this condition, we are preparing to expand our cohort to study children postdrowning acutely, subacutely, and chronically. We encourage other imaging research centers to use the methods herein described to do the same. A concerted, collaborative effort will be needed to determine the prevalence of this condition.

Methodological Considerations

It is important to consider the translation of our image acquisition and analysis methods into the clinical realm. We saw successful application of our protocol on a per-subject basis, allowing for meaningful interpretation and quantification of individual networks in individual patients. Resting-state fMRI during sleep is an ideal paradigm for patients unable to cooperate with traditional task-based or resting-state fMRI scans. Patient contribution, motor response, or comprehension, are not required to probe whole-brain intrinsic activity. From an experimental logistics standpoint, great expertise in administering the scan is not essential [Heine et al. 2012]. ICA is also a voxel-wise, relatively automated network analysis technique that is readily adaptable for clinical use. In our analysis, we fixed the number of components at 20 and otherwise used the software with default parameters. We thus believe the imaging procedure here described to be a readily applicable clinical protocol for use in pediatric drowning, known and suspected disorders of consciousness, and other traditionally difficult patient populations where functional assessments are desirable.

To assess the clinical impact of these methods, we are preparing to apply them more acutely. The optimal timing for implementation of sleep fMRI and ICA network analysis is unknown in pediatric drowning. We hope to investigate their feasibility once patients become stable in the hospital subsequent to the drowning incident. This will provide insight into how soon following the anoxic insult meaningful intrinsic network connectivity can be extracted and analyzed. We additionally aim to determine whether single or multimodal imaging will be optimal in the acute setting. Based on our previous study of white matter pathology in this cohort [Ishaque et al., 2017] and that of Barkovitch et al. [2001] in perinatal ischemia, analyses such as probabilistic tractography across the PLICs using

diffusion-weighted MR data may be more valuable acutely. Future studies should also evaluate longitudinal changes in ICNs and behavioral function in the current cohort. Such investigations could then be extended to address the effects of various interventions on intrinsic connectivity. In chronic ABI patients, functional integrity could be further examined with visual and auditory evoked potentials and event-related potentials to target situational awareness (P300) and language comprehension (N400). Assessment of the potential use of brain–computer interfaces and other genres of communicative devices is also warranted and would further explore our tentative determination that these children have a variant of LIS.

This study is not without limitations. The sample size of 10 patients is admittedly small. Nonetheless, statistically significant results were found both group-wise and per-subject. As mentioned above, an expanded cohort would further improve the imaging–behavioral data correlation analysis and provide insight into the prevalence of this disorder. With ICA decomposition, selection of the dimensionality, or number of components sought from the data, can be arbitrary. We applied a relatively common dimensionality of 20 components, but higher or lower model orders can influence results [Cole et al. 2010; Elseoud et al., 2011; Smith et al. 2009]. Finally, through probing the patient sample with established, normal network architecture, we are assuming the functional network architecture is more-or-less normal. In other words, when a patient network is spatially consistent with the corresponding canonical template, we assume it to be subserving the typical behavioral functions of that canonical network. This may not be the case. To rigorously confirm normal function, one would need to consider task-based fMRI investigation of specific ICN-driven functions.

CONCLUSION

This study demonstrates reduced functional connectivity predominantly limited to motor intrinsic connectivity networks with relative preservation of sensory and some higher-order networks in pediatric ABI from drowning. This pattern of pathology was seen in group-wise and subject-level analyses and was highly concordant with behavioral assessments. Our findings are also consistent with our previously reported structural analyses of grey and white matter pathology, which demonstrated focal, subcortical disruption predominantly affecting motor-system nuclei and tracts. These observations together suggest children with ABI from drowning suffer from a selective deefferentation syndrome, in which motor deficits largely underlie their inability to convey intact cognition and perception. Moreover, our methods for rs-fMRI data acquisition and network analysis proved powerful and should be considered for per-subject, clinical applications.

ACKNOWLEDGMENTS

The Nonfatal Drowning Registry (nonfataldrowningregistry.org) assisted with participant recruitment. The Conrad Smiles Fund (www.conradsmiles.org) publicized this study and provided funding for travel and logistical support. Miracle Flights (miracleflights.org) supported airfare costs. The content is solely the responsibility of the authors and does not necessarily represent the official views of the NIH. The authors thank Thomas Vanasse (UT Health San Antonio) for his guidance in data analysis, and all participants and families for their time and involvement in this study.

CONFLICTS OF INTEREST

Nothing to report.

REFERENCES

Anderson AW, Marois R, Colson ER, et al. (2001): Neonatal auditory activation detected by functional magnetic resonance imaging. Magn Reson Imag 19:1–5

Barkovitch AJ, Westmark KD, Bedi HS, Partrige JC, Ferriero DM, Vigneron DB (2001): Protocol spectroscopy and diffusion imaging on the first day of life after perinatal asphyxia: Preliminary report. Am J Neuroradiol 22:1786–1794.

Baron JC, Bousser MG, Comar D, Castaigne P (1981): "Crossed cerebellar diaschisis" in human supratentorial brain infarction. Trans Am Neurol Assoc 105:459–461.

Bates D, Maechler M, Bolker B, Walker S (2015): Fitting linear mixed-effects models using Ime4. J Statist Software 67:1–48.

Bauer G, Gerstenbrand F, Rumpl E (1979): Varieties of the locked-in syndrome. J Neurol 2221:77–91.

Beckmann CF, Mackay CE, Filippini N, Smith SM (2009): Group comparison of resting-state FMRI data using multi-subject ICA and dual regression. NeuroImage 47:S148.

Beckmann CF, DeLuca M, Devlin JT, Smith SM (2005): Investigations into resting-state connectivity using independent component analysis. Philos Trans R Soc Lond B Biol Sci 360: 1001–1013.

Beckmann CF, Smith SM (2004): Probabilistic independent component analysis for functional magnetic resonance imaging. IEEE Trans Med Imag 23:137–152.

Borse N, Sleet DA (2009): CDC childhood injury report: Patterns of unintentional injuries among 0- to 19-year olds in the United States, 2000. Fam Community Health 32:189–189. 2006.

Broyd SJ, Demanuele C, Debener S, Helps SK, James CJ, Sonuga-Barke EJS (2009): Default-mode brain dysfunction in mental disorders: A systematic review. Neurosci Biobehav Rev 33: 279–296.

Bruno M-A, Schnakers C, Damas F, Pellas F, Lutte I, Bernheim J, Majerus S, Moonen G, Goldman S, Laureys S (2009): Locked-in syndrome in children: Report of five cases and review of the literature. Pediatr Neurol 41:237–246.

Bruno M-A, Vanhaudenhuyse A, Thibaut A, Moonen G, Laureys S (2011): From unresponsive wakefulness to minimally conscious PLUS and functional locked-in syndromes: Recent advances in our understanding of disorders of consciousness. J Neurol 258:1373–1384.

Carrera E, Tononi G (2014): Diaschisis: Past, present, future. Brain 137:2408–2422.

Centers for Disease Control and Prevention (CDC) (2012): Drowning–United States, 2005–2009. MMWR Morb Mortal Wkly Rep 61:344–347.

Childs NL, Mercer WN, Childs HW (1993): Accuracy of diagnosis of persistent vegetative state. Neurology 43:1465–1467.

Cole DM, Smith SM, Beckmann CF (2010): Advances and pitfalls in the analysis and interpretation of resting-state FMRI data. Front Syst Neurosci 4:8.

de Bie HMA, Boersma M, Adriaanse S, Veltman DJ, Wink AM, Roosendaal SD, Barkhof F, Stam CJ, Oostrom KJ, Delemarre-van de Waal HA, Sanz-Arigita EJ (2012): Resting-state networks in awake five- to eight-year old children. Hum Brain Mapp 33:1189–1201.

Demertzi A, Gómez F, Crone JS, Vanhaudenhuyse A, Tshibanda L, Noirhomme Q, Thonnard M, Charland-Verville V, Kirsch M, Laureys S, Soddu A (2014): Multiple fMRI system-level baseline connectivity is disrupted in patients with consciousness alterations. Cortex 42:35–36.

Eliasson A-C, Krumlinde-Sundholm L, Rösblad B, Beckung E, Arner M, Ohrvall A-M, Rosenbaum P (2006): The Manual Ability Classification System (MACS) for children with cerebral palsy: Scale development and evidence of validity and reliability. Dev Med Child Neurol 48:549–554.

Elseoud AA, Littow H, Remes J, Starck T, Nikkinen J, Nissila J, Timonen M, Tervonen O, Kiviniemi V (2011): Group-ICA model order highlights patterns of functional brain connectivity. Front Syst Neurosci 5:37.

Fernández-Espejo D, Soddu A, Cruse D, Palacios EM, Junque C, Vanhaudenhuyse A, Rivas E, Newcombe V, Menon DK, Pickard JD, Laureys S, Owen AM (2012): A role for the default mode network in the bases of disorders of consciousness. Ann Neurol 72:335–343.

Filippini N, MacIntosh BJ, Hough MG, Goodwin GM, Frisoni GB, Smith SM, Matthews PM, Beckmann CF, Mackay CE (2009): Distinct patterns of brain activity in young carriers of the APOE-epsilon4 allele. Proc Natl Acad Sci USA 106:7209–7214.

Fukunaga M, Horovitz SG, van Gelderen P, de Zwart JA, Jansma JM, Ikonomidou VN, Chu R, Deckers RHR, Leopold DA, Duyn JH (2006): Large-amplitude, spatially correlated fluctuations in BOLD fMRI signals during extended rest and early sleep stages. Magn Reson Imag 24:979–992.

Giedd JN, Blumenthal J, Jeffries C, et al. (1999): Development of human corpus callosum during childhood and adolescence: A longitudinal MRI study. Prog Neuropsychopharmacol Biol Psychiatry 23:571–588.

Guttierrez LG, Rovira À, Portela LAP, Leite CDC, Lucato LT (2010): CT and MR in non-neonatal hypoxic–ischemic encephalopathy: Radiological findings with pathophysiological correlations. Neuroradiology 52:949–976.

Heine L, Soddu A, Gómez F, Vanhaudenhuyse A, Tshibanda L, Thonnard M, Charland-Verville V, Kirsch M, Laureys S, Demertzi A (2012): Resting state networks and consciousness: Alterations of multiple resting state network connectivity in physiological, pharmacological, and pathological consciousness States. Front Psychol 3:295.

Hensch TK (2005): Critical period plasticity in local cortical circuits. Nat Rev Neurosci 6:877–888.

Hidecker MJC, Paneth N, Rosenbaum PL, Kent RD, Lillie J, Eulenberg JB, Chester K, Johnson B, Michalsen L, Evatt M, Taylor K (2011): Developing and validating the communication function classification system for individuals with cerebral palsy. Dev Med Child Neurol 53:704–710.

Horovitz SG, Fukunaga M, de Zwart JA, van Gelderen P, Fulton SC, Balkin TJ, Duyn JH (2008): Low frequency BOLD fluctuations during resting wakefulness and light sleep: A simultaneous EEG-fMRI study. Hum Brain Mapp 29:671–682.

Howard RS, Holmes PA, Koutroumanidis MA (2011): Hypoxic-ischaemic brain injury. Pract Neurol 11:4–18.

Huang BY, Castillo M (2008): Hypoxic-ischemic brain injury: Imaging findings from birth to adulthood. RadioGraphics 28: 417–617.

Ibsen LM, Koch T (2002): Submersion and asphyxial injury. Crit Care Med 30:S402–S408.

Ishaque M, Manning JH, Woolsey MD, Franklin CG, Salinas FS, Fox PT (2017): White matter tract pathology in pediatric anoxic brain injury from drowning. Am J Neuroradiol 10.3174/ajnr.A5097.

Ishaque M, Manning JH, Woolsey MD, Franklin CG, Tullis EW, Fox PT (2016): Lenticulostriate arterial distribution pathology may underlie pediatric anoxic brain injury in drowning. NeuroImage Clin 11:167–172.

Jenkinson M, Bannister P, Brady M, Smith S (2002): Improved optimization for the robust and accurate linear registration and motion correction of brain images. NeuroImage 17:825–841.

Kelly RE, Jr., Alexopoulos GS, Wang Z, Gunning FM, Murphy CF, Morimoto SS, Kanellopoulos D, Jia Z, Lim KO, Hoptman MJ (2010): Visual inspection of independent components: Defining a procedure for artifact removal from fMRI data. J Neurosci Methods 189:233–245.

Kriel RL, Krach LE, Luxenberg MG, Jones-Saete C, Sanchez J (1994): Outcome of severe anoxic/ischemic brain injury in children. Pediatr Neurol 10:207–212.

Laird AR, Eickhoff SB, Li K, Robin DA, Glahn DC, Fox PT (2009): Investigating the functional heterogeneity of the default mode network using coordinate-based meta-analytic modeling. J Neurosci 29:14496–14505.

Laird AR, Fox PM, Eickhoff SB, Turner JA, Ray KL, McKay DR, Glahn DC, Beckmann CF, Smith SM, Fox PT (2011): Behavioral interpretations of intrinsic connectivity networks. J Cogn Neurosci 23:4022–4037.

Laureys S, Owen AM, Schiff ND (2004): Brain function in coma, vegetative state, and related disorders. Lancet Neurol 3:537–546.

Leon-Carrion J, van Eeckhout P, Dominguez-Morales M (2002): Review of subject: The locked-in syndrome: A syndrome looking for a therapy. Brain Injury 16:555–569.

Levy DE, Caronna JJ, Singer BH, Lapinski RH, Frydman H, Plum F (1985): Predicting outcome from hypoxic-ischemic coma. JAMA 253:1420–1426.

Lu-Emerson C, Khot S (2010): Neurological sequelae of hypoxic-ischemic brain injury. Neurorehabilitation 26:35–45.

Luo C, Li Q, Xia Y, Lei X, Xue K, Yao Z, Lai Y, Martínez-Montes E, Liao W, Zhou D, Valdes Sosa PA, Gong Q, Yao D (2012): Resting state basal ganglia network in idiopathic generalized epilepsy. Hum Brain Mapp 33:1279–1294.

Manning JH, Courchesne E, Fox PT (2013): Intrinsic connectivity network mapping in young children during natural sleep. NeuroImage 83:288–293.

Merabet LB, Pascual-Leone A (2009): Neural reorganization following sensory loss: The opportunity of change. Nat Rev Neurosci 11:44–52.

Merzenich MM, Van Vleet TM, Nahum M (2014): Brain plasticity-based therapeutics. Front Hum Neurosci 8:385.

Monti MM, Vanhaudenhuyse A, Coleman MR, Boly M, Pickard JD, Tshibanda L, Owen AM, Laureys S (2010): Willful modulation of brain activity in disorders of consciousness. N Engl J Med 362:579–589.

Mundkur N (2005): Neuroplasticity in children. Indian J Pediatr 72:855–857.

Murphy K, Fox MD (2017): Toward a consensus regarding global signal regression for resting state functional connectivity MRI. NeuroImage https://dx.doi.org/10.1016/j.neuroimage.2016.11.052.

Munson S, Schroth E, Ernst M (2006): The role of functional neuroimaging in pediatric brain injury. Pediatrics 117:1372–1381.

Owen A (2017): Into the Grey Zone. New York: Scribner.

Palisaono R, Rosenbaum P, Walter S, Russell D, Wood E, Galuppi B (1997): Development and reliability of a system to classify gross motor function in children with cerebral palsy. Dev Med Child Neurol 39:214–223.

Peltier SJ, Kerssens C, Hamann SB, Sebel PS, Byas-Smith M, Hu X (2005): Functional connectivity changes with concentration of sevoflurane anesthesia. Neuroreport 16:285.

Petrella JR, Provenzale JM (2012): MR Perfusion Imaging of the Brain. Am J Roentgenol 175:207–219.

Plum F, Posner JP (1966): The Diagnosis of Stupor and Coma. 1st ed. Philadelphia, PA, USA: FA Davis.

Plum F, Posner JB (1982): The Diagnosis of Stupor and Coma. 3rd ed. Philadelphia, PA, USA: FA Davis.

Power JD, Mitra A, Laumann TO, Snyder AZ, Schlaggar BL, Petersen SE (2014): Methods to detect, characterize and remove motion artifact in resting state fMRI. NeuroImage 84:320–341.

Pu Y, Li Q-F, Zeng C-M, Gao J, Qi J, Luo D-Z, Mahankali S, Fox PT, Gao J-H (2000): Increased detectability of alpha brain glutamate/glutamine in neonatal hypoxic-ischemic encephalopathy. Am J Neuroradiol 21:203–212.

Rabinstein AA, Resnick SJ (2009): Practical Neuroimaging in Stroke. Elsevier Health Sciences.

Rafaat KT, Spear RM, Kuelbs C, Parsapour K, Peterson B (2008): Cranial computed tomographic findings in a large group of children with drowning: Diagnostic, prognostic, and forensic implications. Pediatr Crit Care Med 9:567–572.

Raichle ME, MacLeod AM, Snyder AZ, Powers WJ, Gusnard DA, Shulman GL (2001): A default mode of brain function. Proc Natl Acad Sci USA 98:676–682.

Raichle ME (2015): The brain's default mode network. Annu Rev Neurosci 38:433–447.

R Core Team (2017): R:A language and environment for statistical computing. R Foundation for Statistical Computing. Vienna, Austria. URL https://ww.R-project.org/.

Redcay E, Courchesne E (2008): Deviant functional magnetic resonance imaging patterns of brain activity to speech in 2–3-year-old children with autism spectrum disorder. Biol Psychiatry 64:589–598.

Robinson S, Basso G, Soldati N, Sailer U, Jovicich J, Bruzzone L, Kryspin-Exner I, Bauer H, Moser E (2009): A resting state network in the motor control circuit of the basal ganglia. BMC Neurosci 10:137.

Rocha-Ferreira E, Hristova M (2016): Review article plasticity in the neonatal brain following hypoxic-ischaemic injury. Neural Plasticity 1–16.

Rosazza C, Minati L (2011): Resting-state brain networks: Literature review and clinical applications. Neurol Sci 32:773–785.

Sellers D, Mandy A, Pennington L, Hankins M, Morris C (2014): Development and reliability of a system to classify the eating and drinking ability of people with cerebral palsy. Dev Med Child Neurol 56:245–251.

Smith E, Delargy M (2005): Clinical review: Locked-in syndrome. British Medical 330.

Smith SM (2002): Fast robust automated brain extraction. Hum Brain Mapp 17:143–155.

Smith SM, Fox PT, Miller KL, Glahn DC, Fox PM, Mackay CE, Filippini N, Watkins KE, Toro R, Laird AR, Beckmann CF (2009): Correspondence of the brain's functional architecture during activation and rest. Proc Natl Acad Sci USA 106:13040–13045.

Szewczyk-Krolikowski K, Menke RAL, Rolinski M, Duff E, Salimi-Khorshidi G, Filippini N, Zamboni G, Hu MTM, Mackay CE (2014): Functional connectivity in the basal ganglia network differentiates PD patients from controls. Neurology 83:208–214.

Tavor I, Parker Jones O, Mars RB, Smith SM, Behrens TE, Jbabdi S (2016): Task-free MRI predicts individual difference in brain activity during task performance. Science 352:216–220.

Topjian AA, Berg RA, Bierens JJLM, Branche CM, Clark RS, Friberg H, Hoedemaekers CWE, Holzer M, Katz LM, Knape JTA, Kochanek PM, Nadkarni V, van der Hoeven JG, Warner DS (2012): Brain resuscitation in the drowning victim. Neurocrit Care 17:441–467.

Vaishnavi SN, Vlassenko AG, Rundle MM, Snyder AZ, Mintun MA, Raichle ME (2010): Regional aerobic glycolysis in the human brain. Proc Natl Acad Sci 107:17757–17762.

Vanhaudenhuyse A, Noirhomme Q, Tshibanda LJF, Bruno MA, Boveroux P, Schnakers C, Soddu A, Perlbarg V, Ledoux D, Brichant JF, Moonen G, Maquet P, Greicius MD, Laureys S, Boly M (2010): Default network connectivity reflects the level of consciousness in non-communicative brain-damaged patients. Brain 133:161–171.

Vincent JL, Patel GH, Fox MD, Snyder AZ, Baker JT, Van Essen DC, Zempel JM, Snyder LH, Corbetta M, Raichle ME (2007): Intrinsic functional architecture in the anaesthetized monkey brain. Nature 447:83–86.

Vlassenko AG, Vaishnavi SN, Couture L, Sacco D, Shannon BJ, Mach RH, Morris JC, Raichle ME, Mintun MA (2010): Spatial correlation between brain aerobic glycolysis and amyloid-β (Aβ) deposition. Proc Natl Acad Sci USA 107:17763–17767.